Nuclear Instruments and Methods in Physics Research A 342 (1994) 516–520
North-Holland

NUCLEAR
INSTRUMENTS
& METHODS
IN PHYSICS
RESEARCH
Section A

Gas scintillation in $He-N_2-CH_4$ and $He-N_2$ mixtures

W. Lorenzon *, O. Häusser, T. Plettner
TRIUMF, 4004 Wesbrook Mall, Vancouver, B.C., Canada V6T 2A3

(Received 11 August 1993; revised form received 8 November 1993)

A gas scintillation time projection chamber has been constructed to measure light emission in $He-N_2-CH_4$ and $He-N_2$ gas mixtures in the pressure range of 5 to 10 atm. N_2 admixtures were on the order of 0.6–1.8% and CH_4 admixtures varied between 0.06–0.18%. It is shown that in this range, an increase in N_2 and CH_4 admixtures tends to decrease the light amplification. The information gained here might be useful for measurements of neutrino angular correlations via the triton asymmetry following muon capture by polarized muonic ^{3}He.

1. Introduction

Over the past two decades gas scintillation proportional counters (GSPC) have been utilized in a wide variety of different applications [1,2]. As a detector, the GSPC has a number of important features such as good energy resolution, high efficiency, and good background rejection efficiency. In recent years, the GSPC has found a new application: the use as an "active target" [3]. For this purpose, the GSPC serves both as gas scintillation detector and as gas target for nuclear physics experiments.

We have adopted this idea to study the possibility of determining the direction of recoils emitted following muon capture on ^{3}He. In this experiment [4] the (μ^- ^{3}He) ion is polarized by direct spin exchange from optically pumped Rb within the μ^- lifetime, and the neutrino angular correlation is to be determined from the triton asymmetry. The triton asymmetry, which is sensitive to the induced pseudoscalar form factor g_p of the semileptonic weak interaction, is to be measured with the gas scintillation time projection chamber (GSTPC).

The choice of the triton detection method compatible with the harsh environment necessary for producing polarized Rb vapor (180°C) is of critical importance. A GSTPC has been chosen over a conventional TPC because it offers the advantage of obtaining precise position information without introducing a large number of feedthroughs into a hot reaction vessel.

Extensive studies on proportional scintillation in argon, krypton and xenon dominated gas mixtures have been performed [5–10], however, very little data is available on helium. Since helium emits light at λ = 60–100 nm gas admixtures have to be added to shift the wavelength to the near UV. Tasiaux et al. [11] have studied ^{3}He dominated gas mixtures at PSI. They used typically 10% Xe admixtures and obtained very clean triton spectra from muon capture on ^{3}He. We decided on N_2 admixtures which is needed for efficient optical pumping of Rb (collisional radiationless deexcitation of the $5P_{1/2}$ excited state of Rb). The emission spectrum of vibrational transitions $C^3\Pi_u \rightarrow B^3\Pi_g$ in N_2 (337, 357, 380 and 406 nm) has been studied extensively [6,8] for mixtures of $Ar-N_2$ and $Ar-CH_4-N_2$. Since emission of the UV light involves the rates of up to nine competing molecular reactions (the corresponding rates for He mixtures are not known) the yield dependence on pressure and concentration of the gas constituents has to be determined empirically. The present study was carried out at room temperature to obtain a cursory overview of the GSTPC properties. Measurements of the temperature dependence of the light output of the GSTPC are being studied at present and will be reported elsewhere.

2. Experimental procedure

The experimental apparatus is shown in Fig. 1. It consists of a stainless steel cross with two UV windows (quartz and fused silica), HV and gas feedthroughs. After pumping the system down to typically 10^{-6} Torr it was filled with premixed gas at pressures up to 10 atm. A windowless ^{241}Am source followed by a 0.85 cm long collimator was used to produce α particles of small opening angles ($\leq 7.5°$) and energy spreads of

* Corresponding author.

SSDI 0168-9002(93)E1264-X

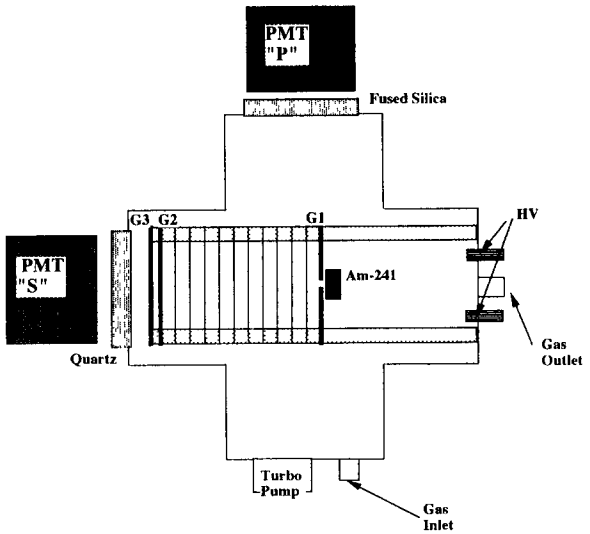

Fig. 1. Schematic diagram of the gas scintillation time projection chamber.

less than 1%. The track lengths for the 5.5 MeV α particles are comparable to those for 1.9 MeV tritons at the same helium pressure. An α particle emitted from the source slows down and stops in the gas producing along its track both scintillation light and ionization electrons. The primary scintillation light was observed in the photomultiplier tube "P", perpendicular to the track. The ionization electrons move in the drift field region between plane G_1 and G_2 to the high-field region between G_2 and G_3, which is referred to as "light gap". In the light gap the ionization electrons are accelerated, producing many secondary photons in successive electron–atom collisions. This secondary scintillation light was observed in the photomultiplier tube "S". It was found that the light amplification is strongly dependent on pressure, gas composition and the electric field applied to the gas.

The drift region was 11 cm long and included a set of field shaping wires equally spaced and interconnected by 10 MΩ resistors. The wire planes in the light gap were 3.1 mm apart and consisted of 127 μm thick beryllium–copper wires, with wire spacings of 0.79 mm. The direction of the drift field (5 kV/11 cm = 455 V/cm) was parallel to the α particle tracks and the secondary light produced in the light gap was observed along the α track in the photomultiplier tube "S". The large ionization density at the end of an α track arrives at the light gap first. This gives rise to the time structure of the secondary light which has a characteristic Bragg distribution, shown in Fig. 2, containing information on the direction of the α track.

3. Results

The shape of the Bragg curve is in qualitative agreement with expectations. The width of the Bragg peak of about 10 μs is proportional to the length of the α track in the drift field and allows a determination of the drift velocity v_{drift}. A more reliable measurement of v_{drift} was obtained from the time delay between prompt primary photons and the least intense part of the Bragg distribution which corresponds to the distance between G_1 and G_2. Typical results for 11 cm drift at different pressures and drift fields are shown in

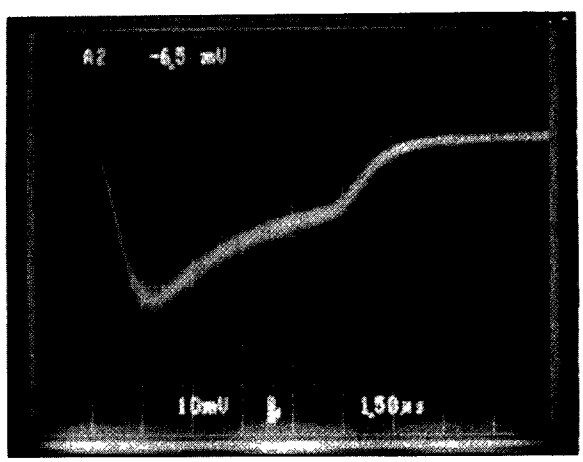

Fig. 2. Secondary light pulse shape of α particles observed in the GSTPC, showing a characteristic Bragg shape. Additional time dispersion caused by diffusion and the finite opening angle of the α particles.

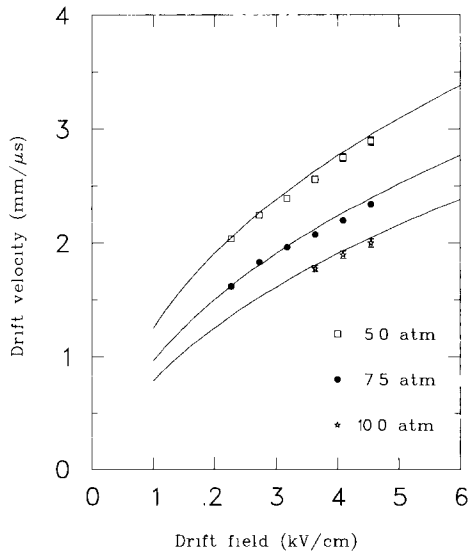

Fig. 3. Drift velocity in GSTPC as a function of drift field for He–N_2 gas mixtures. The N_2 concentration was 1.2%.

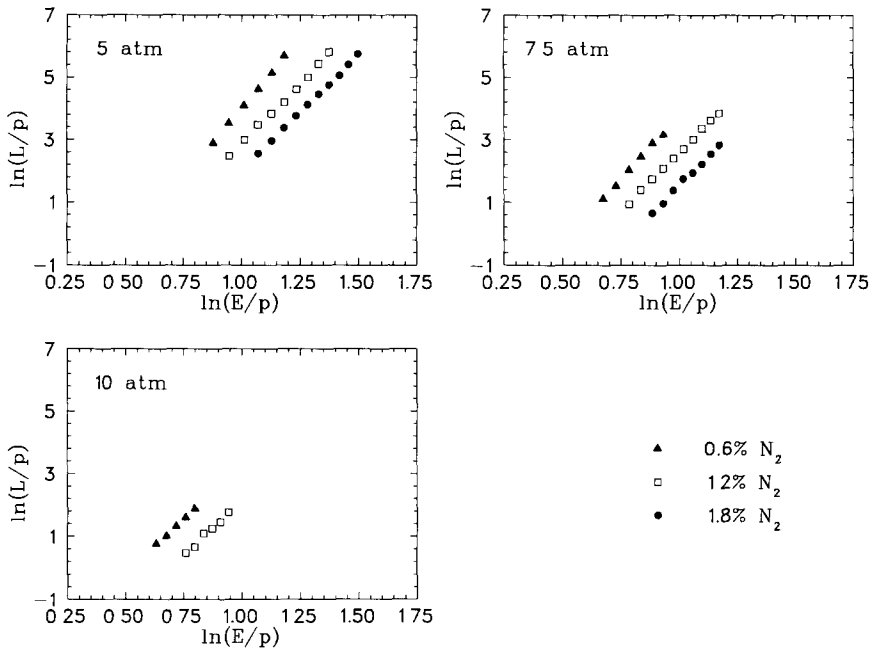

Fig. 4. Reduced light yield versus reduced electric field for He–N_2 gas mixtures.

Fig. 3 and compared with calculations [12]. We found no significant dependence on N_2 concentration, which is in good agreement with these calculations. The variation in v_{drift} over the measured range in N_2 concentration is smaller than 1%.

The reduced yield of UV photons, obtained by

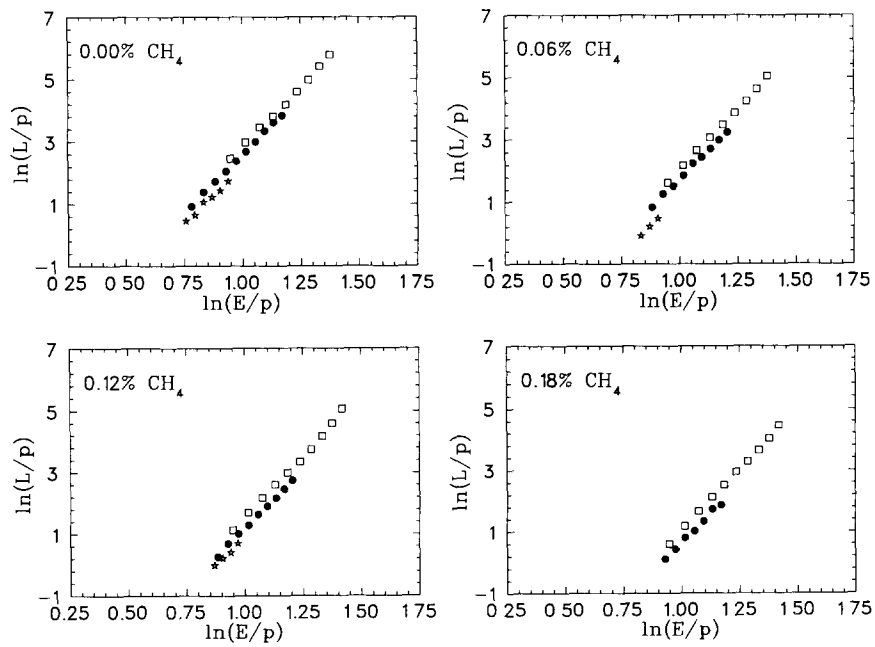

Fig. 5. Reduced light yield versus reduced electric field for He–N_2–CH_4 gas mixtures, with open squares: 5 atm, filled circles: 7.5 atm and stars: 10 atm. The N_2 concentration was 1 2%.

integrating the Bragg curve, is shown in Fig. 4 for N_2 concentrations between 0.6% and 1.8%. It is common to display the data in units of reduced light yield L/p (number of photons produced in light gap/Torr) versus reduced electric field E/p (V cm^{-1} Torr^{-1}), and a linear relationship between L/p and E/p is expected [7]. In this representation the data should show no additional dependence on pressure [13].

In Fig. 5 it is shown that the reduced light yield L/p, apart from its dependence on E/p, is also pressure dependent. A similar effect has been reported in ref. [14]. Fig. 5 also displays the influence of adding 0.06–0.18% of CH_4 to the He–N_2 gas mixture. This has been investigated, because Tasiaux et al. have mentioned that is was necessary to add very small amounts of methane ($< 0.1\%$) to the He–N_2 mixture in order to get stable drift conditions. No such problems have been observed in our system at N_2 concentrations $\geq 1.2\%$. However, at N_2 concentrations below 0.6% the gas mixture tends to light up if the voltage is close to the breakdown point. This effect is due to hard UV photons which are responsible for the creation of secondary photoelectrons, either in the photosensitive gas or in the metallic electrodes. These photoelectrons produce again photons which will be reabsorbed, resulting in positive photon feedback and causing the chamber to become totally inoperable. For more details see refs. [15,16].

As the N_2 concentration is decreased, the system becomes increasingly more unstable, and the maximum electric field, where no breakdown or photon feedback occurs, gets smaller with smaller N_2 admixtures. However, the reduced light yield drops sharply with N_2 concentration for a fixed reduced electric field. Fig. 4 shows this feature at all pressures, in qualitative agreement with ref. [15].

A weighted least squares fit of the type $L/p = a_1(E/p)^{a_2}p^{-a_3}$, $a_{1,2,3}$ being free parameters, was made to the He–N_2 and He–N_2–CH_4 data. This is a modification of the commonly used expression $L/p = a_1(E/p)^{a_2}$ [7], taking into account the additional pressure dependence. The values of the fit are given in Table 1. The common feature for He–N_2 and He–N_2–CH_4 gas mixtures was that the exponent of E/p, (a_2), seems to be roughly independent of the admixed gas concentration. However, the explicit pressure dependence of L/p, (a_3), increases with both the N_2 and CH_4 concentrations, respectively. A drop of the reduced light yield with quencher concentration has been found such that the He–N_2 and He–N_2–CH_4 data could be fitted to a semi-empirical global expression $L/p = a_1(E/p)^{a_2}p^{-a_3}(a_4)^C$, with C the quencher concentration in (%). The fitted parameters are: $a_1 = 82.8 \pm 12.5$, $a_2 = 7.67 \pm 0.11$, $a_3 = 0.85 \pm 0.07$, $a_4 = 0.163 \pm 0.003$ and $\chi^2_\nu = 2.1$ for He–N_2, and $a_1 = 17.8 \pm 1.9$, $a_2 = 7.70 \pm 0.10$, $a_3 = 0.94 \pm 0.07$, $a_4 = (4.20 \pm 0.08) \times 10^{-5}$ and $\chi^2_\nu = 2.4$ for He–N_2–CH_4. It has been attempted, assuming the two quencher gases can be treated independently, to fit all the available data with one general expression

$$L/p = a_1(E/p)^{a_2}p^{-a_3}(a_4)^{C_1}(a_5)^{C_2},$$

with C_1 and C_2 the N_2 and CH_4 concentration in (%), respectively. The fit parameters yielded $a_1 = 172.3 \pm 0.5$, $a_2 = 7.60 \pm 0.08$, $a_3 = 0.93 \pm 0.05$, $a_4 = (2.18 \pm 0.03) \times 10^{-5}$, $a_5 = 0.16 \pm 0.04$, and $\chi^2_\nu = 2.92$ (assuming purely statistical uncertainties). The largest contributions to the systematic uncertainties originate in the accuracy of the pressure gauge used (a 1% error in pressure results in an 8% change in the signal) and the high voltage power supply (2%). Therefore, if a systematic uncertainty of 5% is included in the fit, χ^2_ν reduces to 0.90.

Table 1
Results of a weighted least squares fit with the function $L/p = a_1(E/p)^{a_2}p^{-a_3}$ for the He–N_2 and He–N_2–CH_4 gas mixtures

Gas admixture N_2 [%]	CH_4 [%]	a_1	a_2	a_3	χ^2_ν
0.6	–	0.41 ± 0.04	8.54 ± 0.19	0.37 ± 0.11	2.3
1.2	–	12.69 ± 0.70	7.54 ± 0.11	0.84 ± 0.07	1.1
1.8	–	37.36 ± 0.29	7.44 ± 0.07	1.10 ± 0.06	0.42
1.2	0.06	25.13 ± 0.21	7.72 ± 0.11	0.97 ± 0.07	0.7
1.2	0.12	4.44 ± 0.08	7.95 ± 0.12	0.98 ± 0.08	0.9
1.2	0.18	11.49 ± 0.14	7.91 ± 0.10	1.16 ± 0.07	0.5

The self-absorption of secondary light in the gas at 5 atm has been studied by varying the distance between G_3 and the UV exit window. For two different gas mixtures (1.2% N_2 and 0.6% N_2 + 0.1% CH_4) we found attenuations of about 1.3%/mm. The losses of ionization electrons in the drift region have been measured by changing the length of the drift region (from 6 to 11 cm). This showed that attenuation at 5 atm appears to be negligible for pure N_2 admixtures, and about 5%/cm if 0.1% of CH_4 is added.

The primary scintillation light yield was measured as a function of N_2 concentration in the He–N_2 mixtures. It showed only little dependence on N_2 admixtures, decreasing by about 10% for increasing N_2 admixtures.

The primary charge yield at 5 atm is estimated to be 1.5×10^5 electrons for the α particle entering the drift region. The number of photoelectrons in the photomultiplier tube was obtained by comparing the charge in the Bragg distribution with that for single photon events. Although the wavelength domain in which the measurements of the light emission have been performed was not measured directly, the spectral sensitivity can be estimated from the characteristics of the

photomultiplier tube and the quartz window used. Since quartz transmits light in the range of 170 to 2000 nm, the spectral sensitivity is limited to the spectral response of the EMI9849QB photomultiplier tube which has a quantum efficiency larger than 20% in the range of 180 to 450 nm. By correcting for self-absorption in the gas, quantum efficiency of the photomultiplier tube (25%) and solid angle subtended by the photocathode (530 msr) it is estimated that about 1.4×10^6 UV photons are produced in the light gap. This results in a gain of about 10 UV photons per drift electron in the α track for a gas mixture of 98.8% He + 1.2% N_2 at 5 atm and an electric field of 14.4 kV/cm. This is much lower than numbers quoted in the literature for other gas mixtures ($\approx 10^4$, in Ref. [6]). The energy resolution has a large contribution from photon statistics. The best resolution, about 6.5% full width half maximum, was always observed a few 100 V below the breakdown voltage.

The studies presented here show that N_2 admixtures necessary for optical pumping of Rb (50–100 Torr are typically necessary to quench fluorescence from the $P_{1/2}$ excited state of Rb, see ref. [17]) are compatible with the detection via gas scintillation of charged particles depositing a few MeV in the detector volume. Our studies have shown that impurities have to be kept at a low level (e.g. $\lesssim 10$ ppm of oxygen) to avoid deterioration of the detector performance. A high temperature version of the present setup has been constructed.

Acknowledgements

We would like to thank J. Graham and P. Hauser for initial help with the setup, and W. Cummings, B. Larson and R. Henderson for many fruitful discussions. We gratefully acknowledge the help of the Detector Development Facility group for helping with the design of the GSTPC.

References

[1] M.R. Sims et al., Nucl. Instr. and Meth. 221 (1984) 168.
[2] F. Sauli, Nucl. Instr. and Meth. A 323 (1992) 1.
[3] J. Egger et al., Helv. Phys. Acta 57 (1984) 292.
[4] TRIUMF proposal E683 (1992) unpublished.
[5] M. Suzuki and S. Kubota, Nucl. Instr. and Meth. 164 (1979) 197.
[6] O. Siegmund et al., IEEE Trans. Nucl. Sci. NS-28 (1981) 478;
O. Siegmund, Thesis, University College London (1982).
[7] M. Salete et al., Nucl. Instr. and Meth. 198 (1981) 587
[8] T. Takahashi et al., Nucl. Instr. and Meth. 205 (1983) 591.
[9] S.S. Al-Dargazelli et al., Nucl. Instr. and Meth. 180 (1981) 497.
[10] M. Simon and T. Braun, Nucl. Instr. and Meth. 204 (1983) 371.
[11] B. Tasiaux et al., Particle World, vol. 2 (1991) 81;
B. Tasiaux, Thesis, U.C. Louvain (1992).
[12] G. Schultz, Thesis, University of Strasbourg;
G. Schultz and J. Gresser, Nucl. Instr. and Meth. 151 (1978) 413.
[13] C.A.N. Condé et al, Nucl. Instr. and Meth. 140 (1977) 221.
[14] G. Manzo et al., Nucl. Instr. and Meth. 174 (1980) 301.
[15] P. Fonte et al., Nucl. Instr. and Meth. A 305 (1991) 91.
[16] J. Va'vra, Nucl. Instr. and Meth. A 323 (1992) 34.
[17] B. Larson et al., Phys. Rev. A 44 (1991) 3108.